

June 29, 2015

BACHELOR ASSIGNMENT

OPTIMISATION OF THE WHOLE-BODY SPECT PROTOCOL

Authors:

Julian ABBING (*s1328646*)
Sander BOONSTRA (*s1177656*)
Sipke CNOSSEN (*s1236156*)
Sabine KOENDERS (*s1315161*)
Nienke STOKER (*s1284789*)

Science and Technology Faculty (TNW)

Supervisors:

R. van Rheeën *University Medical Center Groningen*
J.K. van Zandwijk *University of Twente*
M.E. Kamphuis *University of Twente*

Abstract

Introduction: In the year 2014, 687 patients underwent a total bone scan in the University Medical Centre Groningen (UMCG). Of these patients 357 were suspected of bone metastases. The UMCG uses planar bone scintigraphy and Single Photon Emission Computed Tomography combined with Computed Tomography (SPECT/CT) to diagnose patients with suspected bone metastases. Establishing a reliable diagnosis of oncological patients is of great importance. With planar bone scintigraphy there is a great chance small metastases will not be detected by a nuclear medicine physician. Whole-body SPECT increases the chance of detecting lesions, but whole-body SPECT has a scan time of three hours. The aim of this study is to develop an optimised protocol for whole-body SPECT to reduce scan time without compromising image quality.

Method: A phantom study was performed using the Jaszczak and NEMA phantom. A two headed Siemens Symbia T16 scanner with a Low Energy High Resolution (LEHR) collimator was used for the data acquisition. Images obtained with the step-and-shoot mode (SSM) were compared with the SPECT images obtained with continuous rotation mode (CM). The images were objective and subjective evaluated. During the objective evaluation three parameters were evaluated: spatial resolution using the modulation transfer function (MTF), signal to noise ratio (SNR) and contrast. For the subjective evaluation employees of the Department of Nuclear Medicine and Molecular Imaging (NMMI) were asked to scale the images on sharpness, contrast and total quality.

Results: A reduction in scan time of 75% was achieved using CM instead of SSM. The objective evaluation shows that images obtained in CM with 40 views and 12 seconds per view are most similar to the current SPECT images. An overall view of the subjective evaluation shows that the CM with 53 views and 9 seconds per view has a quality near the current SPECT.

Conclusion: The acquisition protocol of the whole-body SPECT for patients with suspected bone metastases can be optimised with CM which results in reduced scan time.

Keywords: whole-body SPECT, continuous rotation, step-and-shoot mode, optimisation

CONTENTS

Contents

1	Introduction	2
1.1	University Medical Center Groningen	2
1.2	SPECT and planar bone scintigraphy	2
1.3	Aim of study	2
1.4	Hypothesis	3
2	Method	4
2.1	The phantom study	4
2.2	Subjective evaluation	7
2.3	Objective evaluation	7
3	Results	10
4	Discussion	12
5	Conclusion and Recommendations	14
5.1	Conclusion	14
5.2	Recommendations	14
6	Acknowledgements	15
7	References	16
8	Appendices	18
8.1	Matlab script of objective evaluation	18
8.2	Questionnaire for the subjective evaluation	21
8.3	List of definitions	24
8.4	Protocols	25

1 Introduction

In the year 2014, 687 patients underwent a total bone scan in the University Medical Centre Groningen (UMCG). Of these patients 357 were suspected of bone metastases [1]. The UMCG uses planar bone scintigraphy and Single Photon Emission Computed Tomography combined with Computed Tomography (SPECT/CT) to diagnose the patients. Although these techniques provide good images, the Department Nuclear Medicine and Molecular Imaging (NMMI) of the UMCG has the desire to investigate the options for improvement of the protocol of the whole-body SPECT and/or whole-body SPECT/CT. The aim of this study is to develop an optimised protocol for whole-body SPECT to reduce scan time without compromising image quality.

1.1 University Medical Center Groningen

The UMCG was established in 2005 as a collaboration between the University of Groningen and the Academic Hospital Groningen (AZG). It is one of the largest hospitals in the Netherlands and the largest employer in the Northern Netherlands. More than 10,000 employees are responsible for patient care, medical education and the implementation of cutting-edge scientific research [2].

The NMMI Department is one of the oldest nuclear medicine institutes in the Netherlands, in fact in the world. In the 1960s the first NaI detector for in vivo measurements and later a gamma camera were acquired. The NMMI Department of the UMCG installed the SPECT and SPECT/CT in 2009 [3]. The Department has the following double headed Siemens SPECT gamma cameras: Symbia T16, Symbia T2 and a Symbia S1.

1.2 SPECT and planar bone scintigraphy

A nuclear medicine study involves an intravenously administered compound which is labelled with a radiation emitting radionuclide. The radiolabelled compound is commonly known as a radiotracer or tracer [4]. For bone scintigraphy Technetium-99m (^{99m}Tc) is used as radionuclide. During the decay of ^{99m}Tc , gamma rays of 140 keV are emitted [5]. The energy of these gamma rays is high enough for a significant number of photons to exit the body without being scattered or attenuated. Therefore it can be detected by gamma cameras [4]. The specific tracer makes sure the radioactive isotope finds its way into the skeleton. Especially in places where cell metabolism is high, the tracer will accumulate. With this technique sites with increased bone cell activity are shown [6]. In an oncological setting the increased activity may indicate bone metastases.

To obtain a picture of the distribution of the radiolabelled compound in the body an external radiation detector, gamma camera, is used. For SPECT a gamma camera is used to record the emissions from ^{99m}Tc for image acquisitions [7, 8].

For planar bone scintigraphy an image is obtained by recording the tracers distribution from one particular angle. A two-dimensional (2D) image is created. To obtain a three-dimensional (3D) image the tomographic mode SPECT is used to record data from many different angles around the patient. This image is called a SPECT image [4].

The whole body is divided in five bed positions. Each bed position is equal to the field of view (FOV) of the detector. The size of the FOV is 53.3 x 38.7 cm [9]. There is a whole-body SPECT protocol available in the UMCG but this takes 3 hours to scan (table 3, appendices). SPECT combined with CT is called SPECT/CT. CT is needed for attenuation correction and provides the anatomy reference for SPECT findings [10]. Research from Palmedo et al. shows that the SPECT/CT imaging technique constructs a better image than planar bone scintigraphy [11].

In figure 1 an image overview of the different techniques as described above is shown.

1.3 Aim of study

Establishing a reliable diagnosis of oncological patients is of great importance. When patients undergo planar bone scintigraphy there is a great chance small metastases will not be detected by a nuclear medicine physician [12]. In other words, the patient will be underdiagnosed. Whole-body SPECT increases the detection of metastases, but it has a scan time of three hours. It is incredibly difficult for a patient to lie still for three hours. Therefore the image of lesser quality provided by planar bone scintigraphy is used. For these reasons the UMCG desires a fast whole-body scan which provides high quality images so that a reliable diagnosis can be established. The aim of this study is to develop an optimised protocol for whole-body SPECT to reduce scan time without compromising

1. INTRODUCTION

image quality. Therefore the main question of this study is:

'How can the acquisition protocol of the whole-body SPECT be optimised to reduce scan time without reducing current image quality for patients with suspected bone metastases?'

Sub questions are:

- What is the clinical relevance of whole-body SPECT/CT?
- What are the advantages and disadvantages of the step-and-shoot mode, continuous step-and-shoot mode and the continuous rotation mode relative to each other?
- How should acquisition angles and time be adapted to reduce total scan time for whole-body SPECT?

1.4 Hypothesis

The whole-body scan time can be reduced to around 40 minutes with the same image quality as the conventional SPECT protocol.

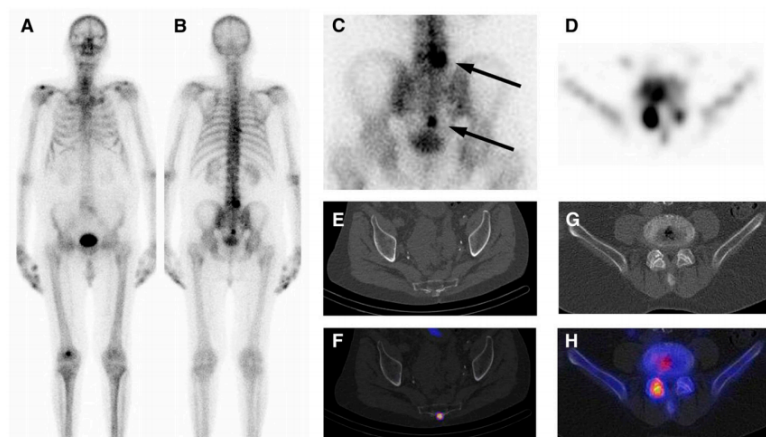


Figure 1: A and B: Planar scintigrams from planar bone scintigraphy. C: Detailed view of pelvis with 2 hot spots (arrows). D: SPECT image, transverse section of upper lesion in lumbar vertebra 5. E: Small osteolytic lesion with intense tracer uptake indicating bone metastases in lower pelvis. E,F,G and H: SPECT/CT, fused image [13].

2 Method

This study was divided into three phases. The first phase included a literature study, the second phase a phantom study and the third phase the evaluation of the acquired data. SPECT has three scan modes: step-and-shoot mode (SSM), continuous step-and-shoot mode (CSSM) and continuous rotation mode (CM). The software of the Symbia T scanner in the UMCG is not able to perform CSSM. Therefore only SSM and CM are included to answer the main question. Using SSM the system only records when the camera is not moving. There is a 'dead time' between every step. When using CM, the camera rotates around the patient with a constant speed and is recording constantly [14]. Data is acquired per set of angles, which can be altered in the protocol settings. Currently the UMCG is using SSM. The biggest advantage of this method is that it has the greatest spatial resolution of all modes [15]. However, this method is slow because the detector stops at every angle to scan. The detector does not scan when moving and therefore it misses counts [14, 16]. The sensitivity of CM is higher than that of SSM. Due to the continuous scanning in CM less counts are missed and due to continuous rotation the detector circles faster around the patient than in SSM. A disadvantage is that CM provides more blurred images [16]. Research from Terrance et al. has shown that there is no significant difference in uniformity and contrast between SSM and CM (when using 3 degrees acquisition). However CM is a lot faster than SSM because of its continuing rotation. It was shown that SSM takes 2.3 minutes per view, while CM takes 1 minute per view [17]. In other phantom studies a reduction of 50% scan time was achieved using 6 degrees acquisition instead of 3 degrees acquisition (figure 2). Using CM another 10% of time could be saved. However this method provided images of lower quality [18]. ZongJian et al. showed that a minimum amount of 31 views in 360 degrees SPECT imaging is sufficient to remove most aliasing artifacts [19].

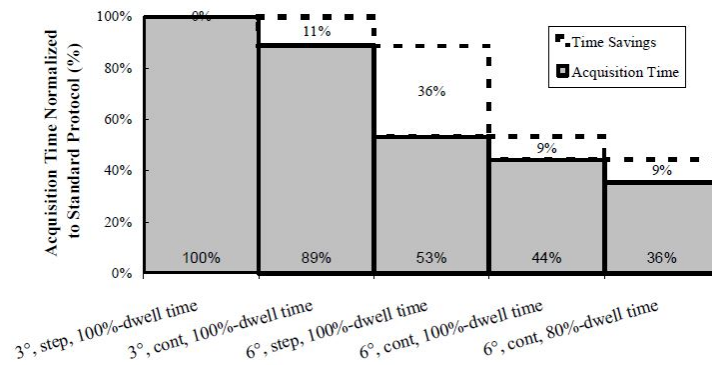


Figure 2: The decrease in acquisition time in myocardial perfusion SPECT imaging using different acquisition methods. Methods used are CM and SSM [18].

2.1 The phantom study

A two headed Siemens Symbia T16 scanner with a Low Energy High Resolution (LEHR) collimator was used for the data acquisition (figure 3). The Jaszczak phantom (figure 4) used in this study is a plexiglass cylinder divided in two sections. The empty cylinder has a volume of 6,9 litre. The lower section contains six sectors of solid plexiglass rods, each sector with its own rod-diameter. These diameters vary from 6,4 mm to 19,1 mm. The distance between the rods is equal to the rod-diameter of the corresponding section. The top section is used to measure the uniformity and the rods section for the spatial resolution. No spheres were inserted in the Jaszczak phantom. Because of the varying size of the rods and the different sectors in which they are placed, the phantom is a 3D 'bar-phantom' [20]. The NEMA phantom (figure 5) is a body shaped plexiglass phantom initially designed for PET. The empty cylinder has a volume of 9,7 litre. It contains a cylindrical insert dimension in the middle with diameter of 51 mm and a length of 180 mm. Which can be filled with styrofoam. Six spheres with diameters varying from 10 mm to 37 mm are located around the cylinder [21]. In this study the spheres were used to calculate the signal to noise ratio (SNR) and contrast. The Jaszczak phantom was filled with a 135 MBq ^{99m}Tc solution. For the NEMA phantom the 135 MBq ^{99m}Tc was diluted so that the ratio of activity in the spheres opposite to the background was four to one. The Jaszczak phantom was placed at the head of the table in the

2. METHOD

middle of the first bed position. The NEMA phantom was placed at the border of two bed positions so possible stitching artifacts could be detected (figures 6 and 7).



Figure 3: Siemens Symbia T16 SPECT scanner, UMCG.

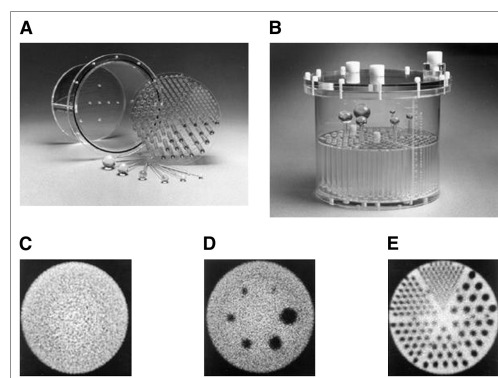


Figure 4: A&B: The Jaszczak phantom, C D&E: reconstructed images of phantom by SPECT [22].

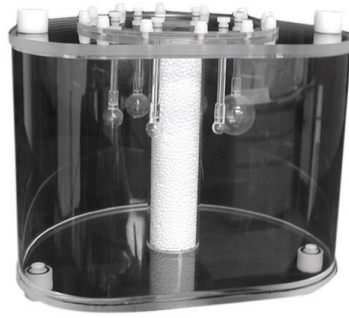


Figure 5: The NEMA phantom [23].

First an image of one FOV was obtained with planar bone scintigraphy and next a SSM SPECT was made. After that the scanning was done using CM following the protocol shown in table 4 in the appendices. This is a modification of the current whole-body SPECT protocol shown in table 3 in the appendices. For a whole-body scan five FOVs must be scanned. At least two bed positions needed to be scanned to see if there were any stitching artifacts. Two FOVs had to be scanned in circa 16 minutes so that a five-FOV-scan would not last longer than 40 minutes. Five scans of two FOVs were made using CM. For each individual scan the angular speed and angle of data acquisition were changed (table 1). While scanning the first bed position each gamma-camera rotated 180 degrees clockwise around the body. During the second bed position the cameras rotated counter clockwise.

After the phantom study the acquired data was evaluated using Matlab for the objective evaluation. The Matlab scripts are included in the appendices. Employees of the NMHI Department were asked to evaluate the images for the subjective evaluation.

Table 1: Total scan time of one bed position with different settings.

Scan method	Scan time of one bed position (minutes)
Current SPECT SSM: 64 views, 15 sec/view	20 minutes
CM: 64 views, 15 sec/view	16 minutes
CM: 64 views, 7 sec/view	7.5 minutes
CM: 32 views, 15 sec/view	8 minutes
CM: 53 views, 9 sec/view	7.95 minutes
CM: 40 views, 12 sec/view	8 minutes

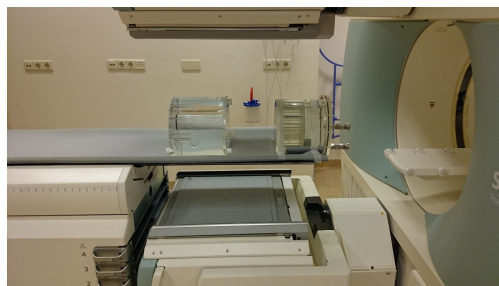


Figure 6: NEMA and Jaszczak phantoms in the SPECT scanner.

2. METHOD

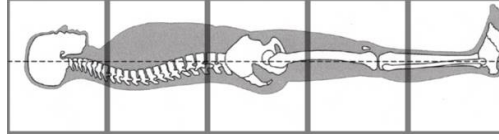


Figure 7: five FOVs for a whole-body scan.

2.2 Subjective evaluation

For the subjective evaluation a questionnaire was given to different employees at the NMMI Department and the University of Twente. This questionnaire contained three SPECT images of each method. The employees did not know which set of images belonged to which method. The first image contained rods of the Jaszczak phantom, the second image spheres of the NEMA phantom and the third image was a coronal view of both phantoms. The questionnaire containing the images can be found in the appendices. Image quality was assessed for three parameters: sharpness, contrast and total quality. The scales ranged from 0 to 10, with 0 for bad, 5 for acceptable and 10 for good. For every employee the mean of each parameter was calculated per set of images. Based on these means the sets were ranged and assigned points from 6 to 1 for respectively highest to lowest mean for all parameters. All points for each method were added and shown in a graph.

2.3 Objective evaluation

Three parameters were calculated to evaluate quality of the images. These were the modulation transfer function (MTF), SNR and contrast.

The MTF defines the ability of SPECT to reproduce an image of an object as a function of spatial frequency [24]. The MTF was calculated using equation 1 [25].

$$MTF = \frac{M_{out}}{M_{in}} = \frac{O_{max} - O_{min}}{O_{max} + O_{min}} \quad (1)$$

M_{in} is the intensity of the real object and M_{out} is the intensity of the image. O_{max} is the highest radiation intensity and O_{min} the lowest [25]. When the MTF has a value of 1, the image is a perfect reproduction of the object. The lower the MTF, the lower the spatial resolution. It is assumed that M_{in} was the same for all methods. Therefore the value has been set to 1 for every method. To calculate M_{out} a line was drawn in transversal slice 59 of the images through rods with the same diameter, respectively 19.1 mm (blue line), 12.7 mm (red line) and 11.1 mm (yellow line) (figure 8). The intensity along these lines was calculated and plotted in a graph (Figure 9). The values of O_{max} and O_{min} were calculated from the graph and used to plot a graph of the MTF.

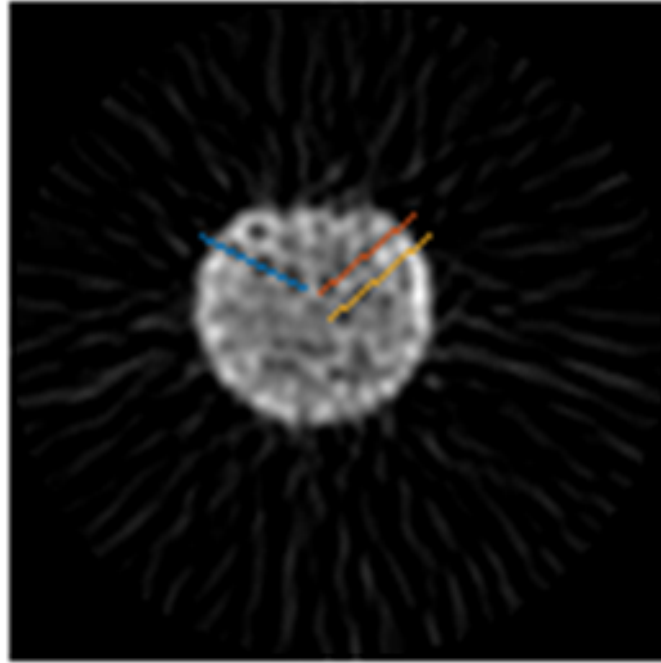


Figure 8: CM with 40 views of 12 seconds per view. Lines used to plot the MTF in slice 59.

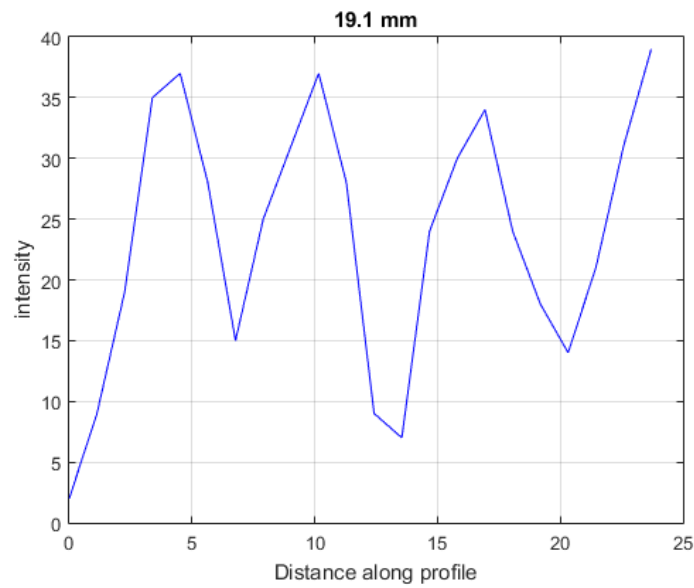


Figure 9: The intensity over the blue line in figure 8. The three local minima between the values 5 and 25 on the x-axis represent the rods.

SNR shows the ratio between the signal and the noise. The ratio is higher when there is less noise in the signal. The SNR was calculated using equation 2 [26].

$$SNR = \frac{Signal}{Noise} \quad (2)$$

A 4x4 matrix in the biggest sphere was used to select an area in the 103th slice of the 'current SPECT' image.

2. METHOD

For all the images the same slice and area with coordinates (61:64,70:73) was used. The mean value in the area was calculated. Noise was calculated using equation 3 of the standard deviation [27].

$$Noise = \sqrt{\frac{\sum (x_i - \bar{x})^2}{n_x}} \quad (3)$$

$$\begin{aligned} x_i &= \text{value of voxel number } i \\ \bar{x} &= \text{mean value of all the voxels} \\ n_x &= \text{total number of voxels} \end{aligned}$$

For multi-headed systems the tomographic contrast is an important indicator for the performance in the detection of small lesions. *Physics in nuclear medicine* provides a general definition of contrast: the ratio of signal change of an object of interest relative to the signal level in surrounding parts of the image [25]. Thus if R_o is the counting rate over normal tissue and R_l is the counting rate over a lesion, the contrast of the lesion was calculated using equation 4 [25].

$$Contrast = \frac{R_l - R_o}{R_o} \quad (4)$$

The contrast was calculated using 4x4 matrices in the background and in the spheres (figure 10) after selecting coordinates of slice 103 in the reference image. The same coordinates for the red (61:64,70:73) and blue (61:64,55:59) matrices were used for all of the images.

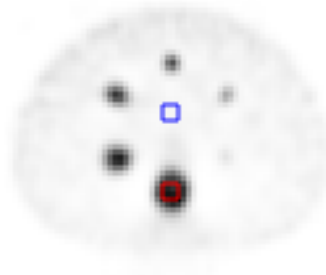


Figure 10: Matrices used to calculate contrast. The blue matrix contains the background and the red matrix contains the sphere.

The results of the subjective and the objective evaluation were compared to each other.

3 Results

The objective evaluation of the phantom study did show differences in all three parameters compared to the current SPECT. Graph 11 shows that the images obtained with the CM methods have higher MTF curves than the current SPECT (CM 64 views 7sec/view, 32 views 15sec/view and 40 view 12 sec/view). Two of the images obtained with the CM methods have almost equal MTF curves to the current SPECT. Table 2 shows the calculated contrast and SNR. The SNR of all images was almost the same. Four of the five new scan methods had a slightly lower SNR. The SNR of the image of CM with 40 views and 12 sec/view was almost equal to the SNR of the current SPECT. The outcome of formula 3 shows that the image of CM with 64 views and 7 sec/view has the lowest contrast, around 50% of the contrast of the current SPECT image. The image of CM with 40 views and 12 sec/view has the highest contrast which is around 89% of the contrast of the current SPECT image.

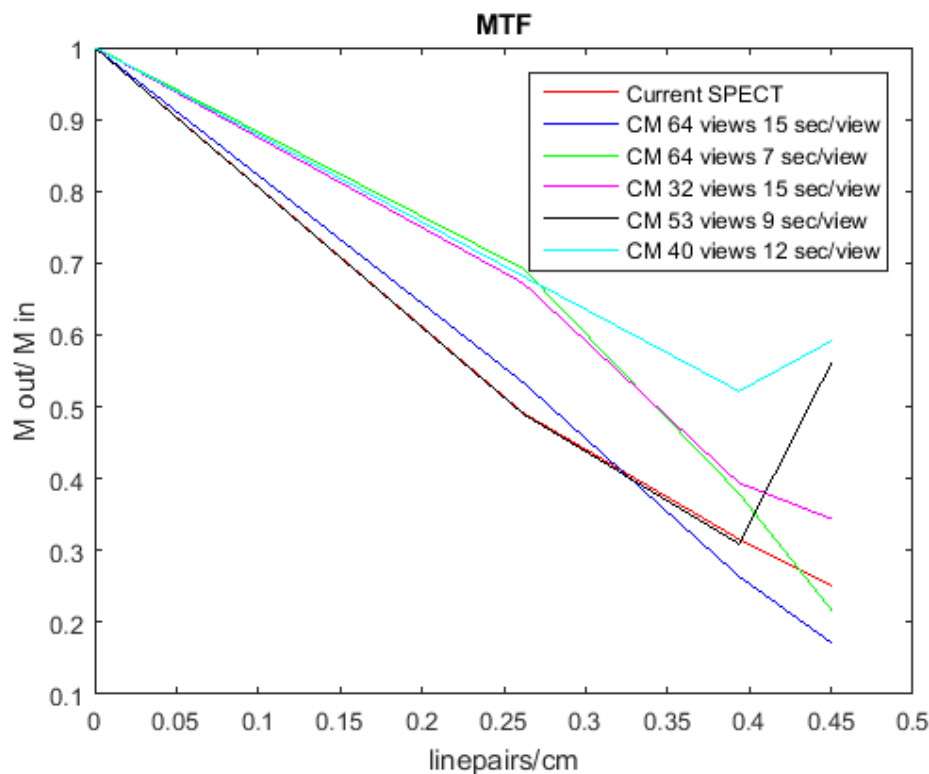


Figure 11: MTF with different scan settings.

Table 2: Contrast and SNR with different number of views and different view times.

Scan	Contrast, 4x4 matrix	SNR, 4x4 matrix
Current SPECT, SSM: 64 views 15 sec/view	22,4246	12,8206
CM: 64 views, 15 sec/view	13,0685	10,3130
CM: 64 views, 7 sec/view	11,1985	10,0838
CM: 32 views, 15 sec/view	11,7560	10,6216
CM: 53 views, 9 sec/view	14,4621	10,3023
CM: 40 views, 12 sec/view	20,0284	12,3171

Using the current protocol, in table 1 called 'current SPECT', 64 views are scanned with 15 seconds per view. Therefore it takes 20 minutes to scan one FOV. Using CM with 64 views and 15 seconds per view, scanning one FOV will take 16 minutes. This is a 20% reduction of scan time. Figure 11 shows a red line which represents the current protocol and a dark blue line which represents the CM with 64 views and 15 seconds per view. CM with 64 views and 15 seconds per view has a better spatial resolution for coarser details and the current protocol

3. RESULTS

for fine details. Scanning with 40 views and 12 seconds per view takes 45 minutes so the time is reduced with 75% relative to the 3 hours of the current protocol for the whole-body SPECT. Images as seen in figure 12 where shown to the employees of the NMMI Department. An overall view of all the subjective evaluations shows that the results of CM with 53 views and 9 seconds per view is almost as good as the results of the current SPECT. The sharpness and total quality are rated higher and the contrast lower in comparison with the current SPECT (figure 13).

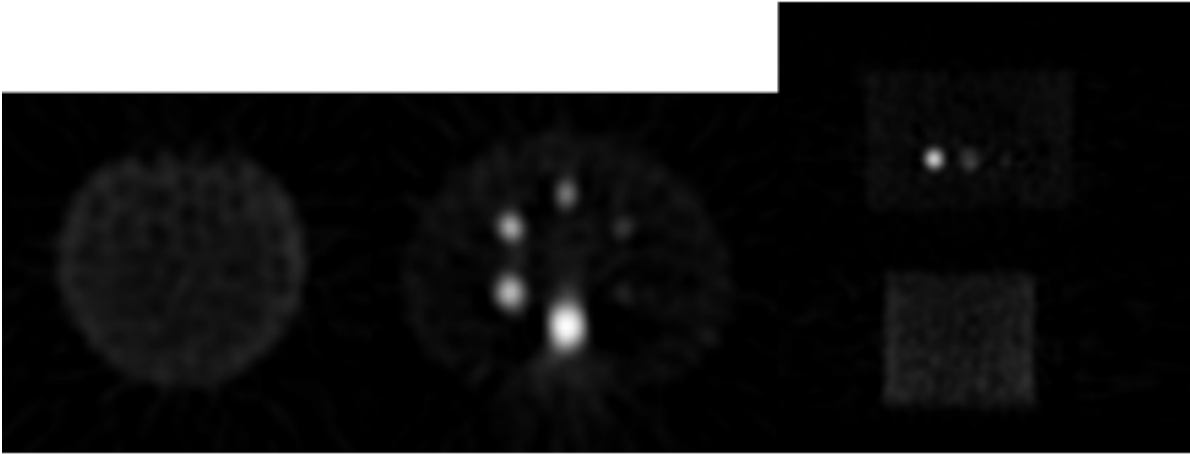


Figure 12: Images given to the employees of the NMMI Department.

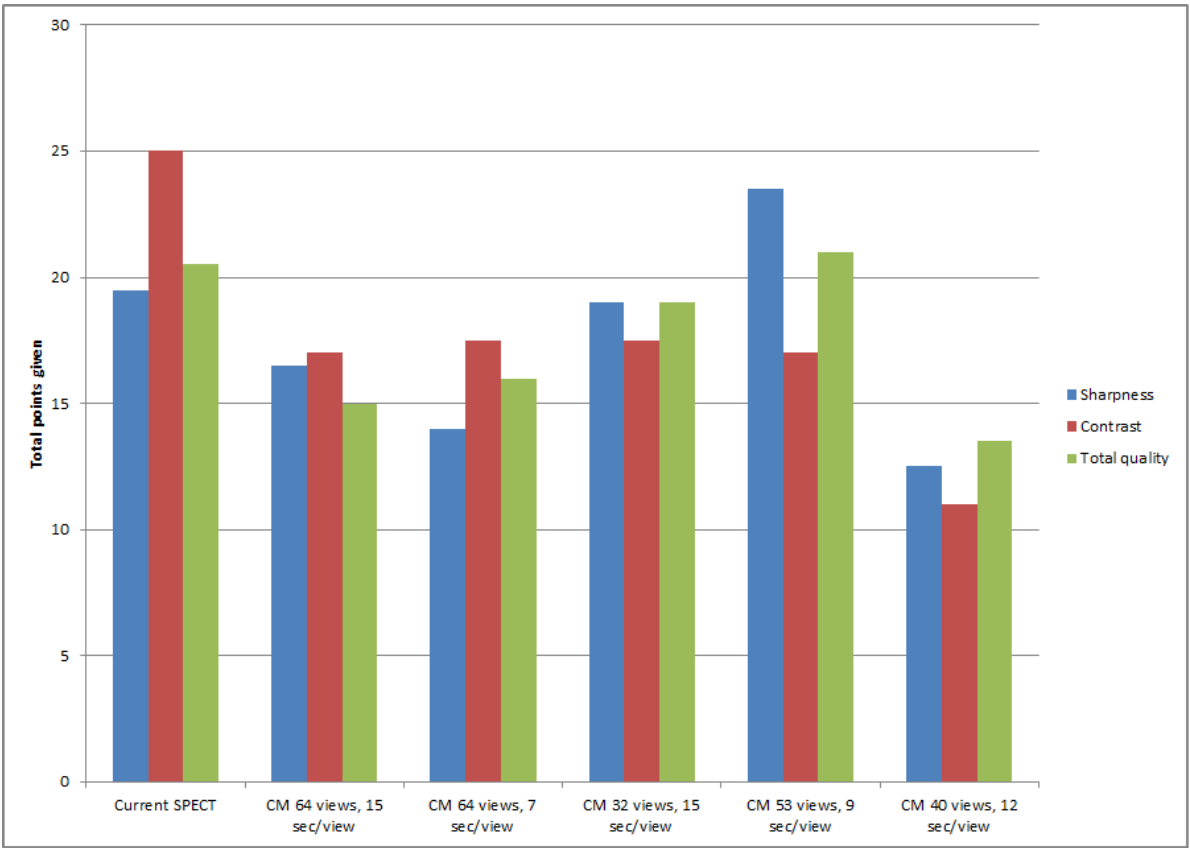


Figure 13: Overall results subjective evaluation.

4 Discussion

CM reduces the scan time of whole-body SPECT. Nuclear medicine physicians now have the opportunity to get an overview of the patients skeleton with possible metastases in 45 minutes. A phantom study with ^{99m}Tc of Bieszk et al. shows that with a decrease of the number of acquisition angles, the resolution and visibility of details becomes less vivid and the number of artifacts increases [16]. Bieszk et al. indicates that for short scans, when the sensitivity is the most important, continuous acquisition is preferred. It provides a big number of views and the best SNR for a fixed scan time [16]. Saad et al. shows that the quality of the SPECT images is limited due to the size of the used matrix. It is shown that there is no significant difference in contrast value when using different matrix sizes in SPECT research. The contrast when using a 128x128 matrix is slightly higher than when using a 64x64 matrix. The count rate when using a 64x64 matrix is higher than when using a 128x128 matrix, because the voxels are larger in a 64x64 matrix. Therefore the voxels are able to catch more counts [28].

Our study was limited by the software of the Siemens Symbia T scanner. Many ideas for reducing scan time could not be tested due to lack of adaptable parameters. Literature shows a scan mode with good opportunities: continuous step-and-shoot (CSSM). The software of Siemens is not capable of applying this mode. CSSM works in the same way as SSM, however in this mode the camera also acquires data when it moves from one position to another. Therefore CSSM will generate images with the sensitivity of CM and the resolution of SSM. In our study the MTF of CM was higher in comparison with SSM. The three lines for the MTF calculation and the matrices for the SNR and contrast were all hand selected. This may have led to a bias in the results. This could be resolved by developing a Matlab script which automatically detects the coordinates that need to be selected for calculating the parameters. CSSM is not faster than SSM, but it does have a better image quality because there will be a higher number of counts. The images made in CSSM are less blurred than images made in CM, because in CSSM the camera does not move for short periods of time. Therefore it will pick up more counts in certain areas. Overall CSSM images will have the best contrast in comparison with SSM and CM, because in this mode the body is scanned in every single angle and even during movement from one angle to another [16].

The total time that covered all the scan methods was circa 6 hours. The half-life time of ^{99m}Tc is 6 hours. The radioactive decay is given by equation 5 [29].

$$A(t) = A_0 e^{-0.693t/T_p} \quad (5)$$

The last scan started about 6 hours after the first scan. Therefore the last scan contained about half of the radioactivity of the first scan. To resolve this problem the phantom study should be divided in two scan moments of three hours, so loss of radioactivity is reduced. It is important that all the variables are equal at the start of each scan moment, for example radioactivity and the positioning of the phantoms. A reference scan should be made during every scan moment using current protocol.

For the subjective evaluation the images were provided in a word-document. This could have reduced image quality. It would have been better if the employees of the NMMD Department and University of Twente evaluated the images with dicomviewers.

Another point of discussion is the clinical relevance of whole-body SPECT. In the UMCG planar bone scintigraphy is the work horse for the detection of bone metastases. This scan method is available in most of the hospitals in the Netherlands. It is relatively cheap and has a high sensitivity for the detection of bone metastases. Unfortunately the high sensitivity correlates with low specificity because lesions by osteoarthritis and infections also lead to higher uptake of radioactive tracers [30]. When the nuclear medicine physician thinks the 2D bone scintigraphy image is insufficient to establish a reliable diagnosis, a 3D SPECT/CT image of the suspicious area is made. The low-dose CT is needed for the attenuation correction and for the anatomical correlation of the SPECT findings during the acquisition and review of the images [31]. Previous studies advice the use of SPECT when planar images are insufficient. In some cases this is even essential [32]. By dividing upper- and lower located radioactivity into tomographical plates, SPECT increases image contrast through reducing background activity positioned over the object activity. Furthermore it enhances the localisation of lesions in comparison with planar bone scintigraphy. More deep and central located lesions are better detected by SPECT than by planar bone scintigraphy. Abnormal heated areas in complex structures like the spine, the hip and the skull base are better detected with SPECT [28, 32]. Especially in the spine it is difficult to detect lesions. When in a variety of clinical settings SPECT imaging was compared with planar imaging, an increase of 20% to 50% in the detection of lesions in the lumbosacral spine was reported [32]. The trans axial images are best for determination of the specific location of the lesion on the vertebrae. These sections are also easy to compare with use of CT [32]. The

4. DISCUSSION

study by Han et al. shows that SPECT gives a higher sensitivity for detection of metastatic tumours compared to planar bone scintigraphy (87% v 74%) and a higher specificity (91% v 81%) [33]. Sedonja et al. gives a sensitivity of 90% for SPECT and 65% for planar scans[34].

As stated before in the UMCG SPECT is combined with a CT image. According to Strobel et al. the visibility of focal lesions is significantly better with SPECT and with SPECT/CT than with planar bone scintigraphy. The research by Strobel et al. states that the sensitivity and specificity for differentiation of benign and malignant bone lesions were 82% and 94% for planar scintigraphy, 91% and 94% for SPECT and both 100% for SPECT/CT. Certainty in diagnosis of a lesion as benign or malignant was significantly higher with SPECT/CT. For planar bone scintigraphy a specific diagnosis was made with an accuracy of 64 %, for SPECT with 86% and 100% for SPECT/CT [30].

Due to the long scan time of the current whole-body SPECT protocol (three hours) used in the UMCG, only a planar whole-body scan is made of the patient. SPECT/CT is only used for the area with suspected bone metastases. Patients are scheduled for 45 minutes to make sure the nuclear medicine physician has time to evaluate the planar image and if needed a SPECT/CT can be made. If there is more than one area suspected of containing bone metastases, the scheduled time is too short to make a SPECT/CT of both areas. Planar bone scintigraphy may be sufficient for the differentiation of malignant and benign lesions but SPECT/CT provides a much higher certainty for a specific diagnosis due to the attenuation correction and the anatomical correlation [30]. Therefore it will be more effective and sufficient to make a whole-body SPECT/CT in the same period of time. This will provide an instant 3D image of the whole body so only one scan is needed for establishing a reliable diagnosis.

Phantoms are not entirely comparable to a human body. All scan methods were used to image the same two phantoms. The images obtained by CM were compared to the image obtained by current SPECT. Current SPECT has already proven to be sufficient to establish a reliable diagnosis on patients. Therefore it is plausible that the CM setting that is superior in the objective and subjective evaluation will provide good images of patients.

5 Conclusion and Recommendations

5.1 Conclusion

The protocol for whole-body SPECT can be optimised by using CM instead of SSM. CM with 40 views of 12 seconds is superior in the objective evaluation. CM with 53 views of 9 seconds comes out on top in the subjective evaluation. Scan time is reduced by 75% compared to the current whole-body SPECT protocol. Therefore a whole-body SPECT can be made in 45 minutes.

5.2 Recommendations

There are two methods which shows to be a good alternative. Both of these methods have to be examined on patients. In our opinion the subjective evaluation outweighs the objective evaluation because a diagnosis is established subjectively. Therefore we recommend CM with 53 views of 9 seconds. A patient study has to be implemented. Every patient has to be scanned twice. The first time with the current protocol and the second time with our protocol. The nuclear medicine physician needs to decide which of the two alternatives is the best method for establishing a diagnosis, that is similar or better to the one that was established using the current SPECT.

Besides CM, a good alternative is CSSM. To implement this method, Siemens has to develop new software which supports this method. This software has to be evaluated using a phantom study. The phantom study can be done following the method used in this study.

No attenuation correction was done in the phantom study. Artifacts which are now present in the images may be reduced by adding CT. However, attenuation correction can also provide artifacts in SPECT [35]. Therefore it is necessary to test this scan method with attenuation correction.

6. ACKNOWLEDGEMENTS

6 Acknowledgements

For the helpful contributions with the technical aspects of this study we want to thank J.K. van Zandwijk and C.H. Slump from the University of Twente. We would also like to thank M.E. Kamphuis from the University of Twente for the support during the whole process. Furthermore, we want to thank Johan de Jong and Tim van der Goot from the University Medical Center Groningen for their help using the SPECT scanner and collecting the data during the phantom study. Finally we would like to express special thanks to Ronald van Rheeën from the University Medical Center Groningen for advising us and providing us this case.

7 References

- [1] UMCG. Department of Nuclear Medicine and Molecular Imaging. *Achieved by nuclear medicine physician Ronald van Rheeën, MD*.
- [2] UMCG. The university medical center groningen. https://www.umcg.nl/EN/corporate/The_University_Medical_Center/Paginas/default.aspx. visited on 22-06-2015.
- [3] UMCG. The university medical center groningen. <https://www.umcg.nl/EN/corporate/Departments/NGMB/research/History/Paginas/default.aspx>. visited on 22-06-2015.
- [4] Simon R Cherry, James A Sorenson, and Michael E Phelps. "What is Nuclear Medicine". In: *Physics in nuclear medicine*. Elsevier Health Sciences. Page 1, 2012.
- [5] Simon R Cherry, James A Sorenson, and Michael E Phelps. "Radionuclide and Radiopharmaceutical Production". In: *Physics in nuclear medicine*. Elsevier Health Sciences. Page 51, 2012.
- [6] A. van Oosterom and T.F. Oostendorp. "Scintigrafie, gammacamera". In *Medische fysica*. Scintigrafie, gammacamera chapter 10.2.2. Elsevier gezondheidszorg. Page 114-115, 2001.
- [7] Simon R Cherry, James A Sorenson, and Michael E Phelps. "the Gamma Camera: Basic Principles". In: *Physics in nuclear medicine*. Elsevier Health Sciences. Page 195, 2012.
- [8] Simon R Cherry, James A Sorenson, and Michael E Phelps. "Single Photon Emission Computed Tomography". In: *Physics in nuclear medicine*. Elsevier Health Sciences. 279-280, 2012.
- [9] Siemens Medical Solutions. Symbia s and t system specifications, 2010.
- [10] B. H. Hasegawa, T. F. Lang, J. K. Brown, E. L. Gingold, and S. C. Blankespoor. Spect reconstruction using uniform and object-specific attenuation maps with emission-transmission ct. In *Nuclear Science Symposium and Medical Imaging Conference, 1992., Conference Record of the 1992 IEEE*, pages 1059–1061 vol.2.
- [11] H. Palmedo, C. Ebert, A. Kreft, B. Marx, Y. Schild, A. Ezziddin, R. Biersack, U. Ahmadzadehfar, H. H. Ko, T. Türler, U. Vorreuther, S. Göhring, H. J. Gerhardt, and H. Pöge. Whole-body spect/ct for bone scintigraphy: Diagnostic value and effect on patient management in oncological patients. *European Journal of Nuclear Medicine and Molecular Imaging*, 41(1):59–67, 2014.
- [12] UMCG. Department of Nuclear Medicine and Molecular Imaging. *Stated by nuclear medicine physician Ronald van Rheeën, MD*.
- [13] A. K. Buck, S. Nekolla, S. Ziegler, A. Beer, B. J. Krause, K. Herrmann, K. Scheidhauer, H. J. Wester, E. J. Rummeny, M. Schwaiger, and A. Drzezga. Spect/ct. *J Nucl Med*, 49(8):1305–19, 2008.
- [14] Zj Cao, C. Maunoury, Cc Chen, and Le Holder. Comparison of continuous step-and-shoot versus step-and-shoot acquisition spect. *J. Nucl. Med.*, 37(12):2037–2040, 1996.
- [15] Salvador T Treves. "Single Positron Emission Tomography". In *Pediatric nuclear medicine*. Springer Science and Business Media. Page 481, third edition, 2013.
- [16] J. A. Bieszk and E. G. Hawman. Evaluation of spect angular sampling effects: Continuous versus step-and-shoot acquisition. *Journal of Nuclear Medicine*, 28(8):1308–1314, 1987.
- [17] T. Chua, H. Kiat, G. Germano, K. Takemoto, G. Fernandez, Y. Biasio, J. Friedman, and D. Berman. Rapid back to back adenosine stress/rest technetium-99m teboroxime myocardial perfusion spect using a triple-detector camera. *Journal of Nuclear Medicine*, 34(9):1485–1493, 1993.
- [18] A. H. Vija, J. Zeintl, J. T. Chapman, E. G. Hawman, and J. Hornegger. Development of rapid spect acquisition protocol for myocardial perfusion imaging, 2006.
- [19] Z. J. Cao, L. E. Holder, and C. C. Chen. Optimal number of views in 360 spect imaging. *Clinical Nuclear Medicine*, 21(2):165, 1996.

- [20] Jennifer Prekeges. *Quality control and artifacts in SPECT*. In: *Nuclear Medicine Instrumentation*. Jones and Barlett Publishers, 2013.
- [21] spect.com. Nema iec body phantom set. http://www.spect.com/pub/NEMA_IEC_Body_Phantom_Set.pdf. visited on 22-06-2015.
- [22] P. Zanzonico. Routine quality control of clinical nuclear medicine instrumentation: a brief review. *J Nucl Med*, 49(7):1114–31, 2008.
- [23] biodex.com. Nema body phantom set http://www.biodex.com/sites/default/files/imagecache/product_landing_large/043-767.jpg. visited on 23-06-2015.
- [24] Raymond A. Applegate. Glenn fry award lecture 2002: Wavefront sensing, ideal corrections, and visual performance. *Optometry and Vision Science*, 81(3):167–177, 2004.
- [25] Simon R Cherry, James A Sorenson, and Michael E Phelps. *Image Quality in Nuclear Medicine*. In: *Physics in nuclear medicine*. Elsevier Health Sciences. 236-243, 2012.
- [26] Simon R Cherry, James A Sorenson, and Michael E Phelps. *Tomographic Reconstruction in Nuclear Medicine*. In: *Physics in nuclear medicine*. Elsevier Health Sciences. 266-268, 2012.
- [27] J.C. van Houwelingen, Th Stijnen, and R van Strik. *Beschrijvende statistiek: tabellen, figuren en kengedaten*. *Inleiding tot de medische statistiek*, volume 2. 2004.
- [28] Ibrahim E Saad, Nadia L Helal, Hazem Mohie El-Din, and Rizk A Moneam. Evaluation of varying acquisition parameters on the image contrast in spect studies. *International Journal of Research and Reviews in Applied Sciences*, 13(2), 2012.
- [29] Simon R Cherry, James A Sorenson, and Michael E Phelps. *Internal Radiation Dosimetry*. In: *Physics in nuclear medicine*. Elsevier Health Sciences. page 410, 2012.
- [30] Klaus Strobel, Cyrill Burger, Burkhardt Seifert, Daniela B. Husarik, Jan D. Soyka, and Thomas F. Hany. Characterization of focal bone lesions in the axial skeleton: performance of planar bone scintigraphy compared with spect and spect fused with ct. *AJR. American journal of roentgenology*, 188(5):W467–474, 2007.
- [31] James A. Patton and Timothy G. Turkington. Spect/ct physical principles and attenuation correction. *Journal of Nuclear Medicine Technology*, 36(1):1–10, 2008.
- [32] Ismet Sarikaya, Ali Sarikaya, and Lawrence E. Holder. The role of single photon emission computed tomography in bone imaging. *Seminars in Nuclear Medicine*, 31(1):3–16, 2001.
- [33] L. J. Han, T. K. Au-Yong, W. C. Tong, K. S. Chu, L. T. Szeto, and C. P. Wong. Comparison of bone single-photon emission tomography and planar imaging in the detection of vertebral metastases in patients with back pain. *Eur J Nucl Med*, 25(6):635–8, 1998.
- [34] I. Sedonja and N. V. Budihna. The benefit of spect when added to planar scintigraphy in patients with bone metastases in the spine. *Clin Nucl Med*, 24(6):407–13, 1999.
- [35] Lynne L Johnson S. James Cullom James A Case James R Galt Ernest V Garcia Keith Haddock Kelly L Moutray Carlos Poston Eli H Botvinick Matthews B Fish William P Follansbee Sean Hayes Ami E Iskandrian John J Mahmarian William Vandeecker Gary V Heller, Timothy M Bateman. Clinical value of attenuation correction in stress-only tc-99m sestamibi spect imaging. *Journal of Nuclear Cardiology*, 11(3):273 – 281, 2004.

8 Appendices

8.1 Matlab script of objective evaluation

```

1  %% MTF
   [A, map]=dicomread('8.IMA');
3  size(A);
   A=squeeze(A);
5  I=A(:,:,59); % one slice is chosen to obtain 2D image
   figure
7  imshow(I,[]); % The image is loaded, every image one by one
   title('CR 40 views, 12 s/v')
9  hold on;
   x1=[38 59]; % The x-coordinates of the line through the rods of 19.1 mm
11 y1=[46 57]; % The y-coordinates of the line through the rods of 19.1 mm
   plot(x1,y1); % The line through the rods is plot
13
   hold on;
15 x2=[79 60]; % The x-coordinates of the line through the rods of 12.7 mm
   y2=[42 58]; % The y-coordinates of the line through the rods of 12.7 mm
17 plot(x2,y2);

19 hold on;
   x3=[82 62]; %The x-coordinates of the line through the rods of 11.1 mm
21 y3=[46 63]; %The y-coordinates of the line through the rods of 11.1 mm
   plot(x3,y3);
23 %% Modulation
   figure
25 improfile(I,x1,y1), grid on; % The intensity over the line is plot
   title('16 mm');
27 figure
   improfile(I,x2,y2), grid on;
29 title('12.7 mm');
   figure
31 improfile(I,x3,y3), grid on;
   title('11.1 mm');
33 %% MTF graph
   Omax=1018; % Current SPECT
35 Omin=347; % The maximum and minimum values between the rods in the intensity graph
   are determined in cursormode of every image, three per image
37 Omax1=900;
   Omin1=468;
39 Omax2=902;
   Omin2=540;
41
   mtf=((Omax-Omin)/(Omax+Omin)); %19.1 mm,
43 mtf1=((Omax1-Omin1)/(Omax1+Omin1));% 12.7 mm
   mtf2=((Omax2-Omin2)/(Omax2+Omin2));% 11.1 mm
45
   Omax3=79; % 64 views 15 s/v
47 Omin3=24;
   Omax4=79;
49 Omin4=46;
   Omax5=65;
51 Omin5=46;

53 mtf3=((Omax3-Omin3)/(Omax3+Omin3)); %19.1 mm
   mtf4=((Omax4-Omin4)/(Omax4+Omin4));% 12.7 mm
55 mtf5=((Omax5-Omin5)/(Omax5+Omin5));% 11.1 mm

57 Omax6=44; % 64 views 7s/v
   Omin6=8;
59 Omax7=40;
   Omin7=18;
61 Omax8=45;
   Omin8=29;
63
   mtf6=((Omax6-Omin6)/(Omax6+Omin6)); %19.1 mm
65 mtf7=((Omax7-Omin7)/(Omax7+Omin7));% 12.7 mm

```

8. APPENDICES

```
mtf8=((Omax8-Omin8)/(Omax8+Omin8));% 11.1 mm
67 Omax9=51; % 32 views 15s/v
69 Omin9=10;
Omax10=46;
71 Omin10=20;
Omax11=43;
73 Omin11=21;

75 mtf9=((Omax9-Omin9)/(Omax9+Omin9)); %19.1 mm
mtf10=((Omax10-Omin10)/(Omax10+Omin10));% 12.7 mm
77 mtf11=((Omax11-Omin11)/(Omax11+Omin11));% 11.1 mm

79 Omax12=38; % 53 views 9s/v
Omin12=13;
81 Omax13=36;
Omin13=19;
83 Omax14=50;
Omin14=14;
85 mtf12=((Omax12-Omin12)/(Omax12+Omin12)); %19.1 mm
87 mtf13=((Omax13-Omin13)/(Omax13+Omin13));% 12.7 mm
mtf14=((Omax14-Omin14)/(Omax14+Omin14));% 11.1 mm
89 Omax15=37; % 40 views 12s/v
91 Omin15=7;
Omax16=35;
93 Omin16=11;
Omax17=39;
95 Omin17=10;

97 mtf15=((Omax15-Omin15)/(Omax15+Omin15)); %19.1 mm
mtf16=((Omax16-Omin16)/(Omax16+Omin16));% 12.7 mm
99 mtf17=((Omax17-Omin17)/(Omax17+Omin17));% 11.1 mm

101 i1=2.5/(5*(19.1/10)); % The calculation for the number of linepairs per cm
i2=3.5/(7*(12.7/10));
103 i3=3.5/(7*(11.1/10));

105 i=[ 0 i1 i2 i3 ];
j=[1 mtf mtf1 mtf2]; % The MTFs that belong to one image are plot in one line
107 j1=[1 mtf3 mtf4 mtf5];
j2=[1 mtf6 mtf7 mtf8];
109 j3=[1 mtf9 mtf10 mtf11];
j4=[1 mtf12 mtf13 mtf14];
111 j5=[1 mtf15 mtf16 mtf17];

113 figure
plot(i,j,'r',i,j1,'b',i,j2,'g',i,j3,'m',i,j4,'k',i,j5,'c') % All the MTFs are plot
115 in one figure

117 title('MTF');
xlabel('linepairs/cm');
119 ylabel('M out/ M in');
legend('Current SPECT','CM 64 views 15 sec/view', 'CM 64 views 7 sec/view', 'CM 32 views 15
121 sec/view', 'CM 53 views 9 sec/view', 'CM 40 views 12 sec/view');

123 %% Contrast
[A,map]=dicomread('8.IMA');
125 size(A)
A = squeeze(A);
127 I = A(:,:,103);
%figure
129 imshow(I,[])
colormap gray;
131 cmap = colormap;
cmap = flipud(cmap);
133 colormap(cmap);

135 rectangle('Position',[61,70,3,3],'EdgeColor','r') % Selected matrices are made
```



```

visible on the image
137 rectangle('Position',[61,55,3,3],'EdgeColor','b')

139 %%
hold on
141 spot =[61 70];
I1 = imcrop(I,[spot, 3, 3]); %select part of an image with matrix 4 by 4
143 spot2 = [61 55];
I2 = imcrop(I,[spot2, 3, 3]);
145 C = (mean(I1)-mean(I2))/mean(I2) %Means of the matrices in formula of contrast

147 %% Signal to noise ratio
A=dicomread('8.IMA');
149 size(A)
A = squeeze(A);
151 I = A(:,:,103);
imshow(I,[]);
153 colormap gray;
cmap = colormap;
155 cmap = flipud(cmap);
colormap(cmap);
157 datacursormode on
%%
159 spot = [61 70] % coordinates used
subimg = imcrop(I,[spot, 3, 3]); %select part of an image with matrix 4 by 4
161 subimg=double(subimg(:));
signal= mean(subimg(:));
163 noise=std(subimg(:));
snr=signal./noise % formula for signal to noise ratio

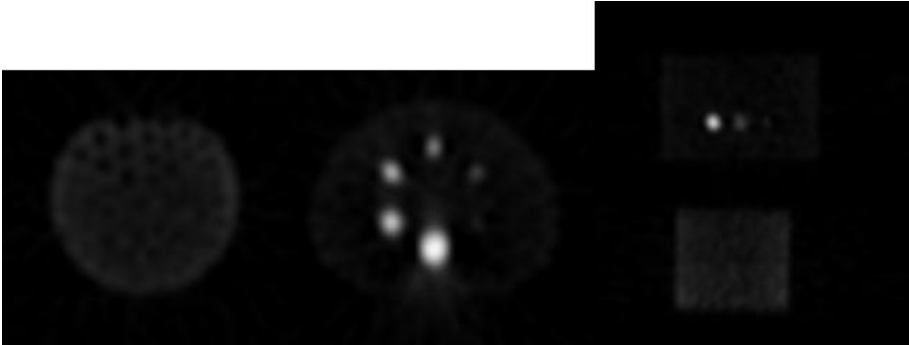
```

8. APPENDICES

8.2 Questionnaire for the subjective evaluation

Function of assessor :

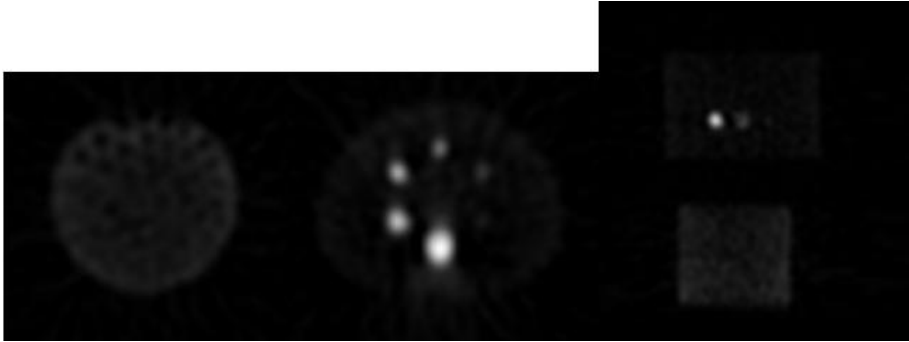
Date:



Scherpte=
Contrast=
Tot. Kwaliteit=

Scherpte=
Contrast=
Tot. Kwaliteit=

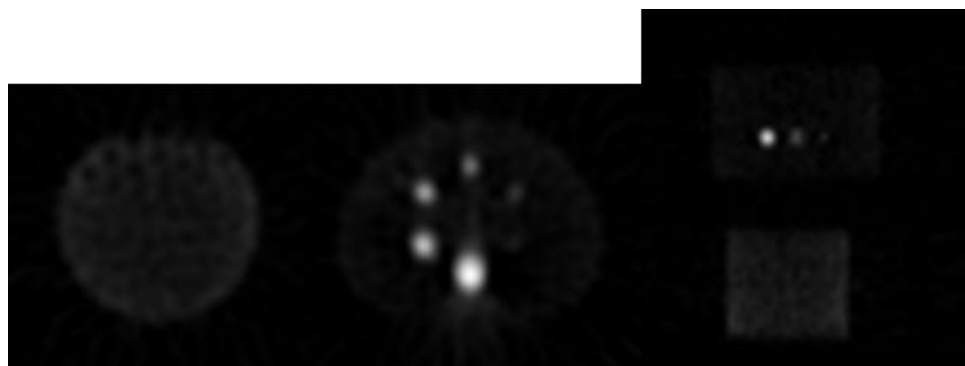
Scherpte=
Contrast=
Tot. Kwaliteit=



Scherpte=
Contrast=
Tot. Kwaliteit=

Scherpte=
Contrast=
Tot. Kwaliteit=

Scherpte=
Contrast=
Tot. Kwaliteit=



Scherpte=
Contrast=
Tot. Kwaliteit=

Scherpte=
Contrast=
Tot. Kwaliteit=

Scherpte=
Contrast=
Tot. Kwaliteit=

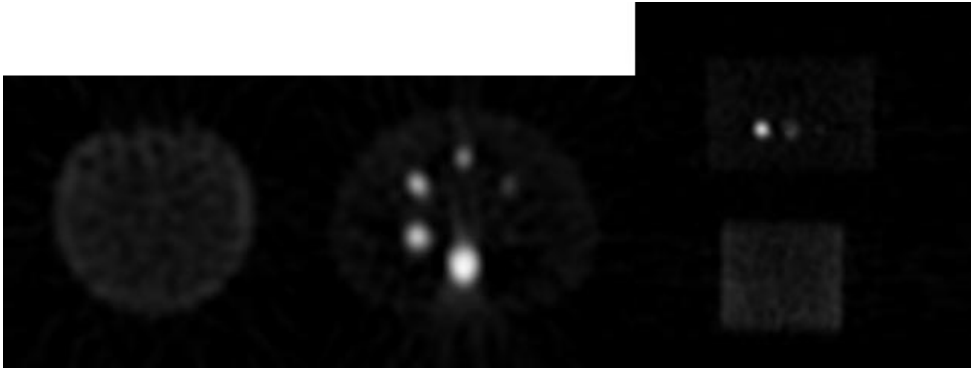


Scherpte=
Contrast=
Tot. Kwaliteit=

Scherpte=
Contrast=
Tot. Kwaliteit=

Scherpte=
Contrast=
Tot. Kwaliteit=

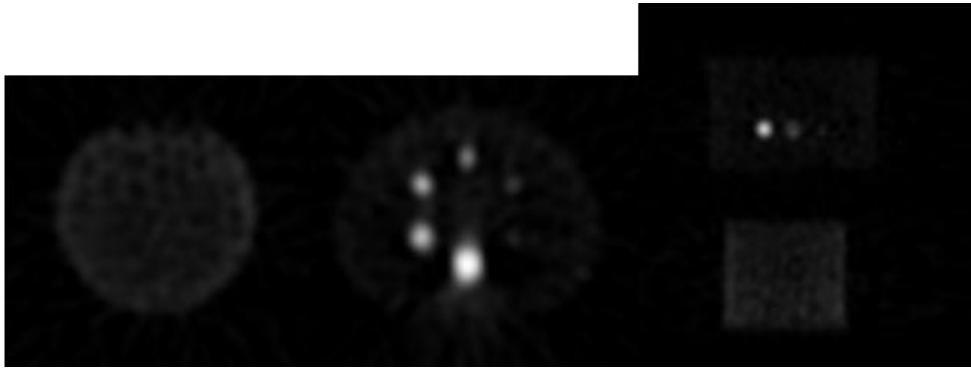
8. APPENDICES



Scherpte=
Contrast=
Tot. Kwaliteit=

Scherpte=
Contrast=
Tot. Kwaliteit=

Scherpte=
Contrast=
Tot. Kwaliteit=



Scherpte=
Contrast=
Tot. Kwaliteit=

Scherpte=
Contrast=
Tot. Kwaliteit=

Scherpte=
Contrast=
Tot. Kwaliteit=

8.3 List of definitions

2D	Two-dimensional
3D	Three-dimensional
^{99m}Tc	Technetium-99m
CM	Continuous mode
CSSM	Continuous step and shoot mode
Contrast	The ratio of signal change of an object relative to the signal level in surrounding parts of the image
CT	Computed Tomography
FOV	Field of view
LEHR	Low Energy High Resolution
MTF	Modulation transfer function
NMMI	The Department of Nuclear Medicine and Molecular Imaging
PET	Positron Emission Tomography
Planar bone scintigraphy	Creates a 2D image
Radioisotope	Radiation emitting radionuclide
Radiotracer	Compound labelled with a radioisotope which is able to find its way to a specific part of the body
SNR	Signal to noise ratio
SPECT	Single Photon Emission Computed Tomography
SSM	Step-and-shoot mode
Tracer	See radiotracer
UMCG	The University Medical Centre Groningen
Whole-body SPECT	Whole-body Single Photon Emission Computed Tomography

8. APPENDICES

8.4 Protocols

Table 3: Current whole-body SPECT protocol from the UMCG

Organ	Skeletal
Isotope 1	99m Technetium , 0,00 mCi, MDP
Matrix Size	128x128
Zoom	1
Camera Preset	Tc99m-NMG
Detectors	Both Detectors
Orientation	Head Out
Patient Position	Supine
Study Based Setup	OFF
Rotation Direction	0
Degrees of Rotation	180
Number of Views	64
Time per View	30 sec
Detector Configuration	180
Orbit	Noncircular
Mode	Step and Shoot
Number of Scans	5
Scan 1 Label	Bed 1
Scan 2 Label	Bed 2
Scan 3 Label	Scan 3
Scan 4 Label	Scan 4
Scan 5 Label	Scan 5
Pause Between Scans	No
Scan direction	Scan Out

Table 4: Continuous rotation protocol, number of views and time per views can be changed. When scanning the whole body the labels can be set to five bedpositions

Organ	Skeletal
Isotope 1	99m Technetium , 0,00 mCi, MDP
Matrix Size	128x128
Zoom	1
Camera Preset	Tc99m-NMG
Detectors	Both Detectors
Orientation	Head Out
Patient Position	Supine
Study Based Setup	OFF
Rotation Direction	0
Degrees of Rotation	180
Number of Views	53
Time per View	9 sec
Detector Configuration	180
Orbit	Noncircular
Mode	Continuous mode
Number of Scans	2
Scan 1 Label	Bed 1
Scan 2 Label	Bed 2
Pause Between Scans	No
Scan direction	Scan In